Stripe Melting in a Two-Dimensional System with Competing Interactions

Antitsa D. Stoycheva and Sherwin J. Singer
Department of Chemistry, The Ohio State University, 120 W. 18th Avenue, Columbus, Ohio 43210
(Received 6 July 1999)

A model with competing short-ranged attractions and long-ranged repulsions that describes self-organized patterns in systems like Langmuir monolayers, magnetic films, and adsorbed monolayers is studied using numerical simulations and analytic theory. Simulations provide strong evidence confirming that the stripe phase order is destroyed in a defect unbinding transition. Large scale computer simulations are in agreement with an analytic scaling theory, which also predicts an eventual crossover from defect-mediated stripe melting to a spin-disordering (or particle-mixing) mechanism with decreasing repulsion strength.

PACS numbers: 68.35.Rh, 05.65.+b, 64.60.Cn, 75.70.Kw

Examples of two-dimensional (2D) systems which exhibit spontaneous modulations are Langmuir monolayers [1], thin magnetic films [2], and physisorbed monolayers on solid surfaces [3]. These systems are diverse at the molecular level, yet the patterns of organization observed—stripes, bubbles, and elongated domains intermediate between stripes and bubbles—show remarkable and fascinating universality. The observed commonality arises because, in all systems mentioned, the self-organized structures are due to a competition between short-ranged attractive forces and long-range repulsions. The repulsive interaction has been demonstrated to originate from actual or effective parallel dipoles in all the experiments mentioned above [4–7], so it decays with distance as R^{-3}.

The observed universality of the self-organized patterns and the fact that the phenomena occur on a length scale much longer than the molecular length scale justify the study of a simplified Hamiltonian which contains the essential ingredients governing self-organization in these systems:

$$-\mathcal{H}/kT = J \sum_{\langle R,R' \rangle} s_R s_{R'} - A \sum_{R,R'} \frac{s_R s_{R'}}{|R - R'|^3} + h \sum_R s_R \,. \tag{1}$$

Besides the domain forming systems already discussed, curvature instabilities of biological membranes [8] have been explained by invoking this model. Elastic forces associated with lattice mismatch between an adsorbed layer and a crystal surface produce very similar domain structures [9], and indeed the elastic case can be regarded as the tensorial generalization of the dipole repulsion problem treated here [10]. From a fundamental scientific viewpoint, the systems listed above provide some of the cleanest experimental realizations of self-organization—"clean" in the sense of having a reasonably simple and well-confirmed microscopic model. However, this model is poorly understood. The phase diagram of the systems governed by the Hamiltonian of Eq. (1) is unknown, and the types of elementary excitations leading to phase transitions are the subject of speculation.

The phase diagrams of models like the one specified in Eq. (1), or continuum versions of the model, have been studied using mean field theory [11,12], or by Brazovskiĭ [13] with a self-consistent approximation. These treatments predict transitions between stripe phases, ordered lattices of bubbles, and isotropic phases. Previous simulations by Hurley and Singer for the dipolar lattice gas model [14] have confirmed that the model of Eq. (1) does support the experimentally observed patterns—stripes, bubbles, and elongated intermediate domains—in the 2D systems of interest. Our present simulations are far more extensive, as described below, and focus on the stripe phase ($h = 0$). In an insightful discussion, Garel and Doniach [11] speculated whether topological defects could provide the mechanism for a Kosterlitz-Thouless (KT) type phase transition [15,16] out of the low-temperature stripe phase. However, their theoretical treatment could not settle the issue and neither could all subsequent theoretical treatments [17–19]. Our results, based on both analytical theory and computer simulations, shed light on this issue for the first time. The answer is that this model supports more than one stripe disordering mechanism, and hence the transition is mediated by topological defects only in a portion of the phase diagram.

The numerical simulations of the model (1) are particularly challenging for several reasons. The interactions are long ranged, and hence the calculation of energy change upon a spin flip in a system of N spins is nominally of order N, unlike the usual Ising model. Lengthy simulations are needed for spin domains to relax and capture an equilibrium ensemble. Phase transitions occur at a temperature which, for our simulations at relative repulsion strength $\eta \equiv \frac{A}{J} = 0.43$, is roughly $\frac{1}{10}$ the value at which the bare Ising model disorders. The Metropolis Monte Carlo (MC) acceptance rate becomes prohibitively small at these low temperatures, and special sampling techniques are required. Finally, to test an analytic result derived below, that the stripe melting temperature rises at small values of η, techniques to handle very large systems are required since the domain length scale explodes exponentially as η

decreases. We pushed our simulations to as small values of η as practical.

In order to carry out the large scale computer simulations needed, we have combined a fast multipole method (FMM), originally proposed by Greengard and Rokhlin [20], and a variant of a non-Metropolis MC sampling technique introduced by Creutz [21]. The essential features of the FMM we have used are the following: (1) the system is divided into a hierarchy of levels; (2) only interactions between spins in close proximity are directly calculated; (3) spins far from the target of a trial move are grouped and a multipole expansion gives the contribution of the group to the interaction field at the target; (4) increasing the distance from the target, the scale of contributing groups increases as well. Our simulations exhibit the expected FMM scaling of CPU time for a MC pass to be $\mathcal{O}(N \ln N)$ as opposed to $\mathcal{O}(N^2)$ in a direct-sum calculation of the interaction potential. The non-Metropolis MC technique we utilized is based on Creutz's microcanonical Monte Carlo algorithm [21]. In the canonical form of the algorithm, trial updates to a group of spins are attempted until an energetically allowed path for the system + thermal demon is found. This allows us to attempt trial moves to many spin configurations per energy calculation, greatly increasing program efficiency at low temperature. Specifically, we attempted updates to one of the 128 possible configurations for hexagonal groups of seven spins on a triangular lattice. Typically, a successful move is found for 30% of the groups visited, far greater than Metropolis Monte Carlo at these temperatures.

We chose a triangular, rather than square, lattice to minimize the influence of the underlying lattice so that our results would apply to continuum systems. Stripe interfaces have lowest energy when aligned along favored directions of the lattice, thereby introducing a p-fold symmetry-breaking orientational field. At low temperatures, José *et al.* [22] showed that these fields are always relevant perturbations. However, their results from an exact duality relation for the Villain model indicate that a p-fold lattice field becomes irrelevant below the Kosterlitz-Thouless transition temperature for $p > 4$, hence our preference for the triangular ($p = 6$) over the square ($p = 4$) lattice [18,19].

Our simulations [23] show clearly demarcated domains in both the ordered and disordered phases (Fig. 1). Hence the transition proceeds via defects in the ordered stripe domains. Visual evidence suggests that the mechanism is a Kosterlitz-Thouless type unbinding of dislocations, present in the oredered phase [Fig. 1(a)], into disclinations, which are seen to proliferate in the disordered phase [Fig. 1(b)]. An order parameter was designed [14] to measure the orientational alignment of the stripe interfaces,

$$g_2 \equiv \left\langle \frac{1}{N} \sum_{\langle R,R' \rangle} \delta_{s_R,-s_{R'}} e^{2i\theta_{R,R'}} \right\rangle, \tag{2}$$

where $\delta_{s_R,-s_{R'}}$ picks out pairs of spins at an interface and $\theta_{R,R'}$ is the angle that a vector joining sites R and R' makes with a reference direction. The stripe melting transition was located by tracking the order parameter as a function of temperature for various values of η and system size, as shown in Fig. 2. The dimensionless heat capacity, $\frac{\partial \langle E/N \rangle}{\partial (k_B T)} = N^{-1}(k_B T)^{-2} \langle (E - \langle E \rangle)^2 \rangle$, is shown as a function of temperature in Fig. 3 through the transition region for several values of the relative repulsion strength, $\eta \equiv \frac{A}{J}$. One of the distinguishing features of the KT mechanism is the absence of a singularity in the heat capacity [15]. The visual evidence of Fig. 1 and the heat capacity data are consistent with stripe melting mediated by topological defect unbinding *for those values of η for which it is practical to perform simulations*. We also attempted to generate data for a finite-size scaling analysis, as has been done to confirm the KT mechanism for other systems [24]. The large number of elementary degrees of freedom per topological defect in our case made the task computationally unfeasible.

The domain interfaces are sharp within the range of η covered by our simulations, as seen in Fig. 1, and overturned spins within a domain are rare. We took advantage of this feature to construct an analytic scaling theory which predicts how the stripe melting temperature should vary with η. With sharp domain interfaces, the energy of the system can be approximated well by line integrals over domain contours $\{C_i\}$, and integrals over domain areas $\{\mathcal{D}_i(C_i)\}$ associated with each contour [5,25]:

$$\mathcal{E}(\{C_i\} \mid A, J) = 4\Big\{ J\gamma \sum_i \int_{C_i} dl + \frac{A}{\sigma^2} \sum_{i<j} \int_{\mathcal{D}_i} d\mathbf{r} \int_{\mathcal{D}_j} d\mathbf{r}' |\mathbf{r} - \mathbf{r}'|^{-3} - \sum_i \frac{A}{2\sigma^2} \sum_i \int_{\mathcal{D}_i} d\mathbf{r} \int_{\substack{\mathcal{D}_i \\ |\mathbf{r}-\mathbf{r}'|>a}} d\mathbf{r}' |\mathbf{r} - \mathbf{r}'|^{-3} \Big\} + \text{const}. \tag{3}$$

In the above expression, σ is the area associated with each spin, $J\gamma$ is the line tension originating from nearest neighbor interactions, a is a microscopic cutoff length, and the energy function $\mathcal{E}$ is in units of $k_B T$. Now we consider a configuration of contours, $\{bC_i\}$, which is identical to the original configuration except that the length scale of all domains is increased by a factor b. The first and second terms in Eq. (3) are easily seen to increase by a factor b compared to their original values. The third term in (3) scales in a nontrivial way, but we can approximate its dependence on b using the energy per domain of perfectly

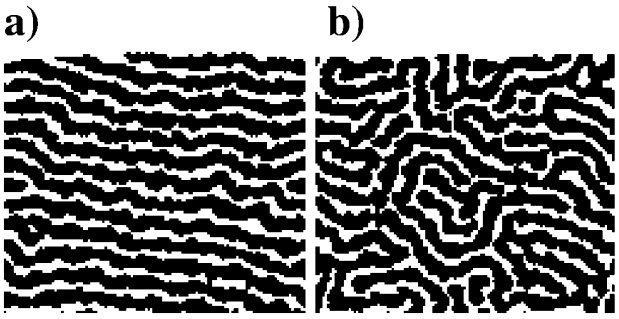

FIG. 1. Typical configurations from the (a) ordered phase ($J = 1.4$) and (b) disordered phase ($J = 1.3$) at relative repulsion strength $\eta \equiv \frac{A}{J} = 0.27$.

straight stripe domains [25]. Now we search for relationships between the original and scaled systems so that

$$\mathcal{E}(\{bC_i\}\,|\,A, J) = \mathcal{E}(\{C_i\}\,|\,A_0, J_0) + \text{const}, \qquad (4)$$

the implication being that the system controlled by parameters (A, J) exhibits the same domain configurations except on a length scale related by the factor b to the original system at (A_0, J_0). In particular, this provides a relationship between the stripe melting point of systems with different values of η.

Using the expression for straight stripe domains in (3) in the regime where domain width is large compared to the lattice spacing, we find that the domain length scale increases exponentially as η decreases,

$$b = \exp\left[\frac{\gamma\sigma^2}{2}\left(\frac{1}{\eta} - \frac{1}{\eta_0}\right)\right], \qquad \left(\eta_0 \equiv \frac{A_0}{J_0}\right), \qquad (5)$$

a result that is expected based on previous studies of domain energetics [5,25], plus a new result that depicts the temperature scaling with η,

$$J = J_0 \exp\left[-\frac{\gamma\sigma^2}{2}\left(\frac{1}{\eta} - \frac{1}{\eta_0}\right)\right]\left(\frac{\eta_0}{\eta}\right). \qquad (6)$$

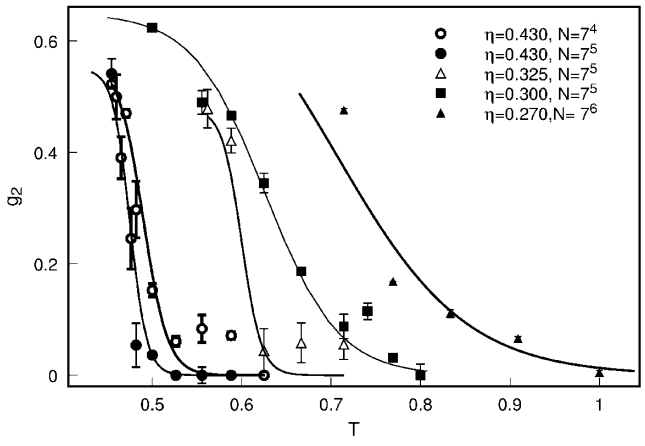

FIG. 2. The twofold order parameter g_2 is plotted as a function of temperature T for several values of $\eta \equiv \frac{A}{J}$. With decreasing repulsion strength, stripes widen and stripe melting temperature shifts upward. The solid lines are drawn as a guide to the eye.

The defect-mediated stripe melting transition is predicted to occur at higher temperature as η is lowered.

The range of validity of expressions (5) and (6) is bounded at large η by the point at which the domain size becomes comparable with the microscopic cutoff a and the continuum expressions lose validity. Far more interesting is the bound at small η. Equations (5) and (6) are valid for sharp domain interfaces. However, as the stripe melting temperature increases according to (6), it will eventually approach the region in which patches of overturned spins appear within the domains, and the system configuration can no longer be specified by a set of contours $\{C_i\}$. When the stripe melting temperature predicted by (6) approaches the bare Ising model critical temperature, we expect that the defect-mediated stripe melting mechanism will be supplanted by disordering of the spins within domains: as temperature is raised the domains will simply fade away before defects destroy stripe order. To test the predictions in (5) and (6) the model must be studied at a range of η values which, as explained earlier, places severe demands on simulation technology.

We have located the stripe melting transition in a range of η values between 0.27 and 0.43 (Fig. 2). Each time we checked for convergence of the stripe melting temperature with system size, except for systems of $7^6 = 117\,649$ spins, the largest simulations performed. Our simulations corroborate the prediction of our analytic theory that stripes widen and stripe melting temperature shifts upward with decreasing repulsion strength, i.e., decreasing η. We present a comparison between T_c predicted by our analytic theory and the values determined in the simulations in Fig. 4. The inset of Fig. 4 indicates the phase diagram implied by our analytic and numerical results: defect-mediated stripe melting moving to higher T or η across the solid phase boundary, and loss of twofold stripe order via disintegration of stripe domains across the dashed

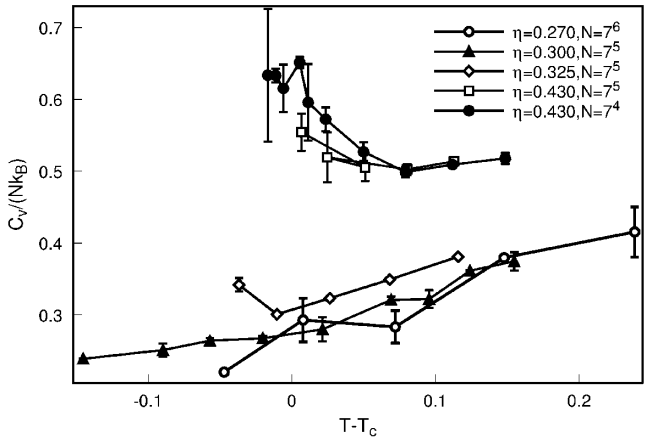

FIG. 3. The dimensionless heat capacity, $\frac{C_V}{Nk_B}$, is shown as a function of temperature difference from the stripe melting temperature for several values of $\eta \equiv \frac{A}{J}$. In agreement with the Kosterlitz-Thouless mechanism, there is no heat capacity anomaly at the transition temperature ($T - T_c = 0$ in these plots).

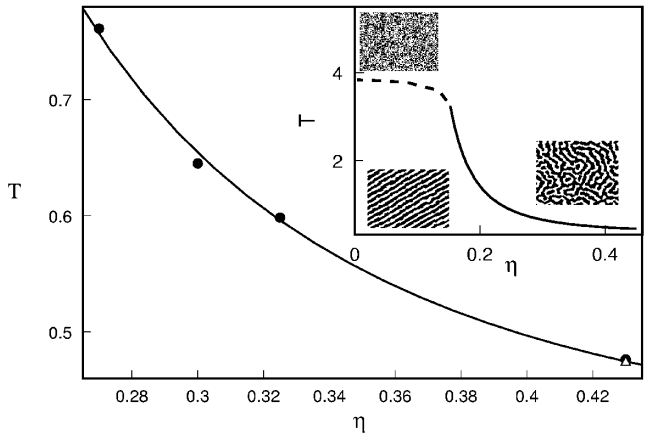

FIG. 4. Stripe melting temperatures predicted by our analytic theory (solid line) and determined from computer simulations (symbols). Two points are plotted for $\eta = 0.43$, corresponding to system sizes of 7^4 and 7^5 spins. The inset shows the phase diagram implied by simulation results and analytic scaling theory.

phase boundary. Observation of the crossover away from defect-mediated stripe melting in our simulations is not feasible; Eq. (6) predicts that the defect-mediated stripe melting point would approach the bare Ising model critical temperature at $\eta \sim 0.14$, necessitating simulations of the order of 10^7 spins. Also in accordance with the scaling notion, energy fluctuations at the stripe melting temperature, as measured by C_V, are independent of η for domains large compared with the lattice, for all but the largest value of η (smallest domains) in Fig. 3.

The results shown in Fig. 4 for the first time explain how compression could induce melting of a Langmuir monolayer stripe phase, as observed by Seul and Chen [26]. Compression decreases the spacing between surface dipoles, increasing the magnitude of dipolar repulsions while weakly affecting the shorter-ranged attractive interactions, increasing η and thereby moving the system from left to right across the phase boundary in Fig. 4. The crossover we predict between defect-mediated stripe melting and non-defect-mediated melting should be experimentally observable by tracking the number of topological defects, the density/magnetization difference in the stripe phase, or the heat capacity. Locating the crossover itself would require a material with a "tunable" effective η. Tuning η might be achieved by chemical or compositional modification in the case of Langmuir monolayers, or modification of materials properties for thin magnetic films.

Acknowledgement is made to the donors of The Petroleum Research Fund, administered by the ACS, for support of this research, and to the Ohio Supercomputer Center for computational resources.

[1] H. Möhwald, Thin Solid Films **159**, 1 (1988).
[2] M. Seul and R. Wolfe, Phys. Rev. A **46**, 7519 (1992).
[3] K. Kern, H. Niehus, A. Schatz, P. Zeppenfeld, J. Goerge, and G. Comsa, Phys. Rev. Lett. **67**, 855 (1991).
[4] C. Kittel, Phys. Rev. **70**, 965 (1946); C. Kooy and U. Enz, Philips Res. Rep. **15**, 7 (1960); A. A. Thiele, J. Appl. Phys. **41**, 1139 (1970); W. A. Barker and G. A. Gehring, J. Phys. C **16**, 6415 (1983); R. E. Rosensweig, M. Zahn, and R. Shumovich, J. Magn. Magn. Mater. **39**, 127 (1983).
[5] D. J. Keller, H. M. McConnell, and V. T. Moy, J. Phys. Chem. **90**, 2311 (1986); H. M. McConnell, P. A. Rice, and D. J. Benvegnu, J. Phys. Chem. **94**, 8965 (1990); S. L. Keller and H. M. McConnell, Phys. Rev. Lett. **82**, 1602 (1999).
[6] W. M. Heckl, H. Baumgärtner, and H. Möhwald, Thin Solid Films **173**, 269 (1989); W. M. Heckl, A. Miller, and H. Möhwald, Thin Solid Films **159**, 125 (1988).
[7] D. Vanderbilt, O. L. Alerhand, R. D. Meade, and J. D. Joannopoulos, J. Vac. Sci. Technol. B **7**, 1013 (1989); D. Vanderbilt, Surf. Sci. Lett. **268**, L300 (1992).
[8] S. Leibler and D. Andelman, J. Phys. (Paris) **48**, 2013 (1987).
[9] V. I. Marchenko, JETP Lett. **33**, 381 (1981); **55**, 73 (1992); O. L. Alerhand, D. Vanderbilt, R. D. Meade, and J. D. Joannopoulos, Phys. Rev. Lett. **61**, 1973 (1988).
[10] D. Vanderbilt, Phys. Rev. B **41**, 7892 (1990).
[11] T. Garel and S. Doniach, Phys. Rev. B **26**, 325 (1982).
[12] D. Andelman, F. Broçhard, and J.-F. Joanny, J. Chem. Phys. **86**, 3673 (1987).
[13] S. A. Brazovskii, Sov. Phys. JETP **41**, 85 (1975).
[14] M. M. Hurley and S. J. Singer, Phys. Rev. B **46**, 5783 (1992).
[15] J. M. Kosterlitz, J. Phys. C **7**, 1046 (1974); J. M. Kosterlitz and D. J. Thouless, J. Phys. C **5**, 124 (1972); **6**, 1181 (1973); Prog. Low Temp. Phys. **7B**, 373 (1978).
[16] J. Toner and D. R. Nelson, Phys. Rev. B **23**, 316 (1981).
[17] A. B. Kashuba and V. L. Pokrovsky, Phys. Rev. Lett. **70**, 3155 (1993); Phys. Rev. B **48**, 10 335 (1993); A. Abanov, V. Kalatsky, V. L. Pokrovsky, and W. M. Saslow, Phys. Rev. B **51**, 1023 (1995).
[18] J. Arlett, J. P. Whitehead, A. B. MacIsaac, and K. De'Bell, Phys. Rev. B **54**, 3394 (1996); I. Booth, A. B. MacIsaac, J. P. Whitehead, and K. De'Bell, Phys. Rev. Lett. **75**, 950 (1995).
[19] Simulations reported in [18] exhibit a heat capacity peak at the stripe melting transition which is not observed in the present work. This may be the result of their use of a square lattice, as discussed in the text, or very small system sizes.
[20] L. Greengard and V. Rokhlin, J. Comput. Phys. **73**, 325 (1987).
[21] M. Creutz, Phys. Rev. Lett. **50**, 1411 (1983); **69**, 1002 (1992).
[22] J. V. José, L. P. Kadanoff, S. Kirkpatrick, and D. R. Nelson, Phys. Rev. B **16**, 1217 (1977).
[23] Animations of our simulations can be viewed at chemistry.ohio-state.edu/~antitsa/Movies.
[24] D. Frenkel and R. Eppenga, Phys. Rev. A **31**, 1776 (1985); A. Alavi, Phys. Rev. Lett. **64**, 2289 (1990), Mol. Phys. **71**, 1173 (1990).
[25] M. M. Hurley and S. J. Singer, J. Phys. Chem. **96**, 1938 (1992); **96**, 1951 (1992).
[26] M. Seul and V. S. Chen, Phys. Rev. Lett. **70**, 1658 (1993).